Enhanced Radiomics for Prediction of Rupture Status in Cerebral Aneurysms

Alexandra Lauric, Calvin G. Ludwig, Adel M. Malek

■ BACKGROUND: **Radiomics is a powerful tool for automatic extraction of morphological features, but when applied to cerebral aneurysms, it is inferior to established descriptors in classifying rupture status. We sought a strategy to recover neck orientation and parent vessel caliber to enhance Radiomics performance and facilitate its adoption for aneurysm risk stratification.**

■ METHODS: **We analyzed 135 sidewall (32 ruptured) and 216 bifurcation (90 ruptured) aneurysms from three-dimensional rotational catheter angiography datasets. Clinical three-dimensional rotational catheter angiography defined in arbitrary orientation underwent affine transformations enabling aneurysm neck alignment to XY plane before analysis in PyRadiomics, facilitating automatic extraction of aneurysm height and width, previously not possible with random alignment. Additionally, parent vessel size was estimated from aneurysm location and incorporated into enhanced Radiomics (height, width, height/width, size ratio). Rupture status classification was compared across methodologies for 31 automatically computed conventional Radiomics, enhanced Radiomics, and established size/shape descriptors using univariate, multivariate, and area under the curve (AUC) statistics.**

■ RESULTS: **Enhanced Radiomics–derived height/width and size ratio were significantly higher in both ruptured subsets. Using multivariate analysis in sidewall lesions, enhanced Radiomics (AUC = 0.85) matched established features (AUC = 0.86) and outperformed conventional Radiomics (AUC = 0.82); in bifurcation lesions, enhanced Radiomics (AUC = 0.78) outperformed both established features (AUC = 0.76) and conventional Radiomics (AUC = 0.74).**

■ CONCLUSIONS: **Enhanced Radiomics incorporating neck orientation and parent vessel estimate is an efficient operator-independent methodology that offers superior rupture status classification for both sidewall and bifurcation aneurysms and should be considered a strong candidate for larger-scale multicenter and multimodality validation.**

INTRODUCTION

PyRadiomics (Radiomics)[1] is a recently introduced automatic imaging processing tool for the evaluation of intensity-based descriptors and shape morphology. Radiomics allows for the evaluation not only of shape, including size, area, and volume, but also of image characteristics, such as patterns and intensity distributions. Radiomics is primarily used for analysis of pathological lesions, and results have been reported on characterization of lung cancer,[2] liver fibrosis,[3] prostate lesions,[4] glioblastoma,[5] metastatic brain tumors,[6] and metastases to the head and neck.[7] Recent research[8-10] has proposed the use of Radiomics-derived morphological descriptors for classification of rupture status and risk stratification of cerebral aneurysms. Aneurysmal subarachnoid hemorrhage is associated with high mortality and morbidity despite advances in management,[11] making identification of potential rupture risk surrogates of high clinical value.

Although the International Study of Unruptured Intracranial Aneurysms (ISUIA) proposed an aneurysm size threshold of 7–10

Key words
- Aneurysm rupture
- Aneurysm shape
- Intracranial aneurysms
- PyRadiomics
- Radiomics aneurysm morphology
- Risk stratification

Abbreviations and Acronyms
2D: Two-dimensional
3D: Three-dimensional
AUC: Area under the curve
ISUIA: International Study of Unruptured Intracranial Aneurysms

Cerebrovascular and Endovascular Division and Cerebrovascular Hemodynamics Laboratory, Department of Neurosurgery, Tufts Medical Center, Tufts University School of Medicine, Boston, Massachusetts, USA

To whom correspondence should be addressed: Adel M. Malek, M.D., Ph.D. [E-mail: amalek@tuftsmedicalcenter.org]

Citation: World Neurosurg. (2021). https://doi.org/10.1016/j.wneu.2021.11.038

Journal homepage: www.journals.elsevier.com/world-neurosurgery

Available online: www.sciencedirect.com

1878-8750/$ - see front matter © 2021 Elsevier Inc. All rights reserved.

mm for surgical management,[12,13] many aneurysms rupture at sizes <7 mm.[14] Additional aneurysmal size and shape features have been considered for rupture risk determination, such as aneurysm height,[15] height-to-width ratio,[16] aneurysm aspect ratio,[17] size-to-vessel diameter ratio,[18] inflow angle,[19] and estimations of shape deviations from ideal spherical or elliptical forms,[20] among others. These features have been previously evaluated on large samples of ruptured and unruptured aneurysms and are well established in the literature. Many of these descriptors are still evaluated through manual measurements; thus, a widely available, operator-independent tool such as Radiomics would be advantageous for improving accuracy and reproducibility of results.

However, as currently used, Radiomics lacks the ability to account for spatial orientation (height, neck position), which hinders its performance in rupture status classification[10]; indeed, it was recently shown to be inferior to established size and shape parameters. The aim of this study was to propose a strategy to enhance Radiomics performance by recovering aneurysm orientation and using a location-dependent parent vessel estimated caliber. This set of enhanced Radiomics descriptors was evaluated on sidewall and bifurcation aneurysms separately because these 2 aneurysm subtypes have been shown to behave differently under morphological evaluation.[21] In particular, bifurcation aneurysms, which account for more than half of all ruptured aneurysms, have proven difficult to classify morphologically.[21] We compared performance of enhanced Radiomics against well-known shape and size descriptors previously established in the literature[17,20,21] and against nonenhanced Radiomics.

MATERIALS AND METHODS

Patient Selection, Angiography, and Data Processing

Consecutive high-resolution three-dimensional (3D) catheter-based cerebral angiograms were obtained using either a Philips Integris (Philips Medical Systems North America Co., Bothell, Washington, USA) or Siemens Artis (Siemens Medical Solutions USA, Inc., Malvern, Pennsylvania, USA) calibrated biplane system with volume reconstruction using the respective clinical software packages to yield a 3D volumetric dataset (Figure 1A). All studies of aneurysms with imaging of sufficient quality to permit accurate image processing and morphological analysis were included. Fusiform aneurysms with no definable neck were excluded from analysis. Clinical information, including rupture status (ruptured/unruptured aneurysms), was retrieved from a prospectively maintained database. All angiographic data for ruptured aneurysms within this set were obtained in emergent fashion and before vasospasm onset.

Because of documented differences in morphology between bifurcation and sidewall aneurysms, the 2 subtypes were analyzed separately.[21] Aneurysms were defined as sidewall lesions if they originated from only 1 parent vessel or from the origin of a branch with a diameter smaller than one fifth the diameter of the parent vessel.[21] Aneurysms were defined as bifurcation lesions if they were located at major dividers in the vasculature. Lesions at the ophthalmic or anterior choroidal artery origins were classified as sidewall aneurysms given the much smaller diameter of the bifurcating vessel compared with the internal carotid artery caliber. Posterior communicating artery lesions were classified as either sidewall or bifurcation aneurysms depending on the size of the posterior communicating artery relative to the internal carotid artery diameter as previously described.[21,22] Volumetric datasets, including aneurysm and

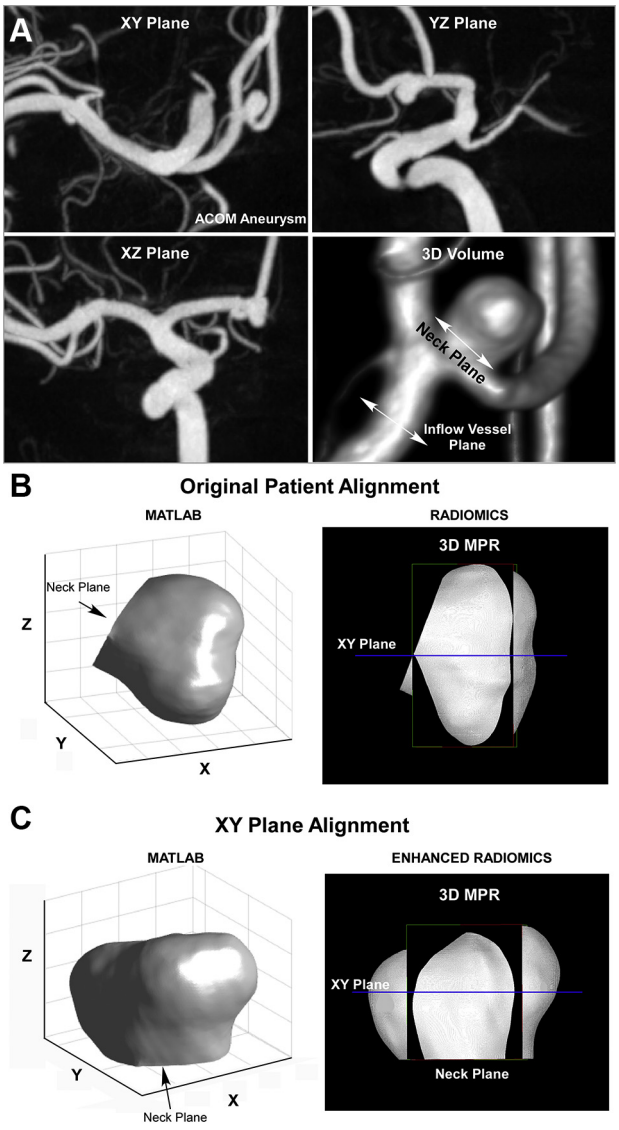


Figure 1. (**A**) Maximum intensity projection in the XYZ coordinate system, including three-dimensional volume rendering showing the neck and inflow vessel plane. (**B**) Angiographic volumes, originally defined in the anatomical coordinate system (axial, sagittal, and coronal), have arbitrary XYZ coordinate placement. (**C**) Before Radiomics evaluation, all models are reoriented in the XYZ coordinate system and, by convention, have the aneurysm neck aligned to the XY plane. ACOM, anterior communicating artery; 3D, three-dimensional; MPR, multiplanar reconstruction.

parent vessel, were segmented using Amira 5.3 software (FEI Company, Hillsboro, Oregon, USA). The aneurysm domes were represented as triangular meshes for further processing.

The research was approved by the institutional review board. Patient consent was waived because of the retrospective nature of the study not impacting patient clinical care.

Aneurysm Orientation Transformations

Angiographic volumes are defined in the anatomical coordinate system (axial, sagittal, coronal), but have arbitrary XYZ placement. As a result, aneurysm computational meshes have arbitrary orientation in the XYZ coordinate system (Figure 1B). Before Radiomics evaluation, all shapes were preprocessed using an in-house MATLAB (The Mathworks, Inc., Natick, Massachusetts, USA) tool that was previously introduced and validated for automatic morphological evaluation of aneurysms.[23] Using this tool, the plane defining the aneurysm neck was automatically detected, and the rotation matrix necessary for XY alignment was evaluated based on the original neck location in the XYZ coordinate system. The resulting shape- and size-preserving transformation was applied to the aneurysm dome, resulting in neck alignment to the XY plane (Figure 1C). This alignment process is automated, reproducible, and suitable for batch processing and enables comparison across all aneurysms using a consistent orientation. Aneurysmal surfaces were voxelized using a MATLAB script such that mesh surfaces were represented as a Digital Imaging and Communications in Medicine volume, enabling input to PyRadiomics feature extraction tool (https://pyradiomics.readthedocs.io/en/latest/).

Enhanced Radiomics Morphological Feature Extraction

A PyRadiomics package implemented in Python was used.[1] Similar to previous work,[8,10] only shape parameters were included in this study, as intensity-derived features are not relevant for 3D rotational catheter angiography data used to generate the aneurysm volumetric representation. Detailed information of Radiomics features is available in the documentation for PyRadiomics (https://pyradiomics.readthedocs.io/en/latest/features.html).

For the purpose of this study, we refer to this shape-only feature group as conventional Radiomics descriptors. 3D Radiomics morphological descriptors were extracted as previously described (Figure 2)[8-10]: Maximum3DDiameter (largest pairwise Euclidean distance between any mesh pairs), MajorAxisLength (largest axis length of the enclosing ellipsoid), MinorAxisLength (second-largest axis length of the enclosing ellipsoid), LeastAxisLength (smallest axis length of the enclosing ellipsoid), Elongation (MinorAxisLength/MajorAxisLength ratio), Flatness (LeastAxisLength/MajorAxisLength ratio), SurfaceArea (total area of the shape), MeshVolume (total volume of the shape), SurfaceVolumeRatio (ratio of surface area to volume of a shape), and Sphericity (a measure of how close the shape resembles a sphere).

The following two-dimensional (2D) measures are also available in Radiomics: Maximum2DDiameterSlice (largest pairwise Euclidean distance between surface mesh vertices in the axial plane), Maximum2DDiameterColumn (largest pairwise Euclidean distance between surface mesh vertices in coronal plane), and Maximum2DDiameterRow (largest pairwise Euclidean distance between surface mesh vertices in the sagittal plane). For originally randomly aligned aneurysms, these 2D descriptors hold no particular meaning in the XYZ coordinate system, as they represent a random slice of the dome volume. However, with the

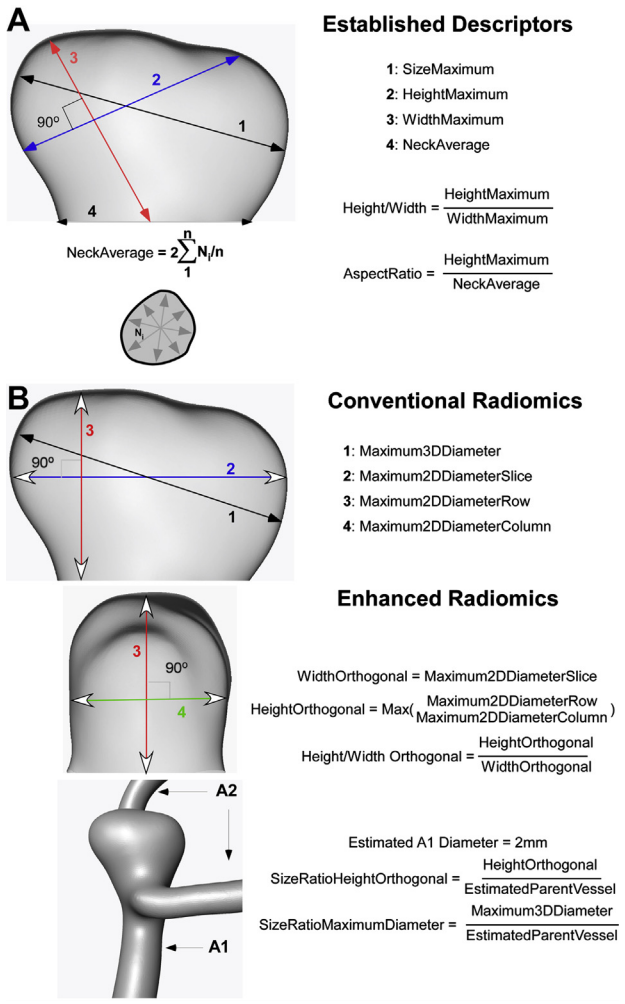


Figure 2. (**A**) Evaluation of established descriptors. The neck plane is shown as a thin horizontal line. SizeMaximum is the maximal diameter of the dome. HeightMaximum is the maximal distance from the neck center to the aneurysm dome. WidthMaximum is the maximal distance orthogonal to HeightMaximum. NeckAverage is computed as twice the average distance from the neck center to neck border. (**B**) Evaluation of conventional Radiomics descriptors. Maximum3DDiameter is the largest pairwise Euclidean distance between any surface mesh vertices. Maximum2DDiameterSlice is the largest pairwise Euclidean distance between surface mesh vertices in the axial plane. Maximum2DDiameterColumn is the largest pairwise Euclidean distance between surface mesh vertices in the coronal plane. Maximum2DDiameterRow is the largest pairwise Euclidean distance between surface mesh vertices in the sagittal plane. For originally randomly aligned aneurysms, these two-dimensional descriptors hold no particular meaning in the XYZ coordinate system, as they represent a random slice of the dome volume. (**C**) With the alignment and placement of aneurysmal neck parallel to the XY plane, HeightOrthogonal and WidthOrthogonal can be evaluated. Size ratio can also be evaluated by use of estimated vessel size based on aneurysm location.

alignment and placement of aneurysmal neck parallel to the XY plane, additional morphological features can be evaluated from these 2D measures: HeightOrthogonal (maximum height orthogonal on the neck plane, as the maximum between Maximum2DDiameterColumn and Maximum2DDiameterRow), WidthOrthogonal (maximum dimension parallel to the neck as the Maximum2DDiameterSlice), and orthogonal Height/Width Orthogonal (HeightOrthogonal/WidthOrthogonal) (Figure 2B).

Prior Radiomics analysis[8-10] was limited to the dome and did not enable size ratio computations, given their need for parent vessel/inflow caliber analysis. We have elected to extend this functionality by using an estimated inflow vessel size from available literature information,[24] based on the given aneurysm location in the cerebral vasculature (Table 1). Consequently, the following features were also evaluated: SizeRatioHeight Orthogonal (ratio between HeightOrthogonal and inflow size) and SizeRatioMaximumDiameter (ratio between Maximum 3DDiameter and inflow size).

Overall, as a result of the neck alignment and inflow estimation described above, Radiomics-derived features were augmented with 5 additional descriptors (height, width, height/width, size ratio height, and size ratio diameter), referred to as enhanced Radiomics.

Table 1. Aneurysm Distribution by Location ($N = 353$)

Aneurysm Location	Number of Aneurysms (%)	Inflow Vessel Size (mm)
ACOM	95 (26.9)	2
MCA	60 (16.9)	2.6
ICA	51 (14.7)	3.9
PCOM	51 (14.5)	3.3
BA	24 (6.7)	2.8
OPTH	24 (6.7)	3.6
ICAB	17 (4.8)	3.4
ACHA	10 (2.8)	3.3
SCA	6 (1.7)	3
ACA	5 (1.4)	2.7
VA	4 (1.1)	2.6
PCA	3 (0.8)	1.3
PICA	2 (0.5)	2.5

ACOM, anterior communicating artery; MCA, middle cerebral artery; ICA, internal carotid artery; PCOM, posterior communicating artery; BA, basilar artery; OPTH, ophthalmic artery; ICAB, internal carotid artery bifurcation; ACHA, anterior choroidal artery; SCA, superior cerebellar artery; ACA, anterior cerebral artery; VA, vertebral artery; PCA, posterior cerebral artery; PICA, posterior inferior cerebellar artery.

Established Size and Shape Feature Extraction

For each segmented surface, the aneurysm dome was isolated from the surrounding vessels and represented as a 3D triangular mesh model using Amira 5.3 (Figure 2A). The process was performed under the supervision of the senior author (A.M.M.), and the integrity of each aneurysm morphology was maintained to the best of our ability. No cases were excluded based on the ability to achieve satisfactory isolation of aneurysms from parent vessels. The corresponding neck plane was defined for each aneurysm and was similarly represented as a 3D triangular mesh model. Similar to other studies in the field,[20,25] the aneurysm neck plane was selected at the location where the dome protrudes outward from the parent vessel.[23] A cross-sectional plane cut was also selected on the inflow parent vessel at a distance of 1 vessel diameter from the aneurysmal neck and was similarly represented as a triangular mesh, used in established parameter computation of size ratio.

Size and shape parameters were automatically extracted from the 3 surfaces (aneurysm, neck plane, parent vessel plane) using a previously described and validated MATLAB script.[23] The features evaluated have been previously described and used in the literature for rupture status classification.[23] For the purpose of this study, we refer to this feature group as established descriptors. They are as follows: SizeMaximum (aneurysm size), HeightMaximum (largest distance between the center of the neck and the aneurysm surface, not necessarily orthogonal to the neck plane), WidthMaximum (largest distance orthogonal to the maximal height), NeckAverage, and ParentVesselSize (size of inflow vessel) (Figure 2A).

These size features were used to evaluate 1) height width (Height/Width) as the ratio HeightMaximum/WidthMaximum, 2) aspect ratio (AspectRatio) as the ratio HeightMaximum/NeckAverage, 3) bottleneck factor (BottleneckFactor) as the ratio WidthMaximum/NeckAverage, and 4) size ratio (SizeRatio) as the ratio HeightMaximum/ParentVesselSize.

Three complex shape parameters—Undulation Index, Ellipticity Index, and Non-Sphericity Index—were evaluated using MATLAB utilizing the formulas introduced by Raghavan et al.[20] Undulation Index captures surface irregularities of the aneurysm wall with lower values being smooth. Ellipticity Index varies from 0 (hemisphere) to 1 being higher for egg- and mushroom-shaped aneurysms. Non-Sphericity Index represents deviation of the shape from a sphere.

To summarize, all morphological features (Radiomics and established) were evaluated in an automated fashion. However, the processing pipeline for evaluating established features includes semiautomatic segmentation and manual selection of neck and vessel planes. To compare performance between established and Radiomics features, same segmentation models were used to evaluate established features and to create the Digital Imaging and Communications in Medicine volume, which represents the input to Radiomics. However, if aneurysm morphology were to be evaluated by Radiomics alone, users would have the option of using the 3D Slicer imaging tool (https://www.slicer.org/)[26] for the entire pipeline of image processing, segmentation, and Radiomics evaluation. Whereas for the evaluation of the established features, patient-specific vessel measurements were used, in the case of Radiomics features we used estimated vessel calibers based on the aneurysm location to maintain the original proposed sparse processing pipeline.

Statistical Analysis

The analysis was performed retrospectively, and the aneurysms were divided into ruptured and unruptured subsets for analysis. JMP Pro 14 software (SAS Institute Inc., Cary, North Carolina, USA) was used to perform Student t test, and multivariate analysis of significant features was performed using stepwise forward selection with significance assumed for $P < 0.05$. Receiver operating characteristic curves were generated and performance evaluated using the area under the curve (AUC).

RESULTS

Patient Demographics

A total of 351 aneurysmal 3D rotational catheter angiography volumes were analyzed with location distribution as detailed in Table 1. There were 135 sidewall aneurysms (32 ruptured; 109 women; age 56.03 ± 14.99 years) and 216 bifurcation aneurysms (90 ruptured; 150 women; age 56.49 ± 14.16 years), with no significant difference in age between ruptured and unruptured aneurysms in either sidewall (Table 2) or bifurcation (Table 3) groups.

Correlation and Differences Between Established and Radiomics Descriptors

Similar to previous work,[10] there was near-perfect correlation between identical established Descriptors measured by MATLAB script and Radiomics pairs of descriptors, such as SizeMaximum and Maximum3Ddiameter ($P < 0.0001$, $R^2 = 0.99$), and between established Volume and Radiomics MeshVolume ($P < 0.0001$, $R^2 = 0.99$).

However, as mentioned before,[10] established parameters are evaluated on the surface segmentation of the aneurysms, and as such surface area evaluation does not include the neck area, but rather represents the area of an open surface as is the case with similar research.[20,25] In contrast, because Radiomics are evaluated on a volumetric segmentation of the aneurysms, parameters are measured on a closed surface, which includes the neck surface. This difference results in an overestimation of the aneurysm area by Radiomics compared with established area (Tables 2 and 3). This area overestimation-results in an underestimation of Radiomics Sphericity and an overestimation of SurfaceVolumeRatio.

Statistical Analysis on Sidewall Aneurysms

Based on literature review, inflow parent vessel diameter was estimated according to aneurysm location (Table 1) and used for size ratio determination as part of the enhanced Radiomics descriptors. Most conventional Radiomics parameters were statistically significant in predicting rupture status (Table 2), but enhanced Radiomics descriptor SizeRatioMaximumDiameter ($P < 0.0001$, AUC = 0.79) was identified as best performing for rupture classification, followed by Maximum3DDiameter ($P < 0.0001$, AUC = 0.77). Ruptured aneurysms had significantly greater size and size ratio compared with unruptured aneurysms (Table 2).

Similarly, all established size and shape parameters except NeckAverage were statistically significant in identifying rupture status in sidewall aneurysms. SizeRatio ($P < 0.0001$, AUC = 0.81), HeightMaximum ($P < 0.0001$, AUC = 0.79), and AspectRatio ($P < 0.0001$, AUC = 0.78) were the best among established parameters. Ruptured aneurysms had significantly larger size ratio, height, and aspect ratio compared with unruptured aneurysms (Table 2 and Figure 3A).

Multivariate statistical analysis was performed using forward feature selection on descriptors that achieved significance in univariate evaluation (Figure 3B). Enhanced Radiomics (Height/Width Orthogonal, Maximum3DDiameter, HeightOrthogonal, MeshVolume, and SurfaceArea) (AUC = 0.85) outperformed conventional Radiomics (AUC = 0.82) and showed similar performance to established descriptors (AUC = 0.86) (Figure 3C). In this sidewall subset, enhanced Radiomics performance depended exclusively on aneurysm and neck orientation rather than on inflow parent vessel size estimation.

Statistical Analysis on Bifurcation Aneurysms

Conventional Radiomics and established descriptors both performed worse on classifying rupture status in bifurcation than sidewall aneurysms. Size descriptors were not statistically significant in discriminating bifurcation rupture status (Table 3). Shape features such as Elongation ($P < 0.0001$, AUC = 0.72) and Flatness ($P < 0.0001$, AUC = 0.73) were the most important conventional Radiomics features. In addition, enhanced Radiomics height/width and size ratio were significantly higher in ruptured bifurcation aneurysms. Similarly, established features were not significantly different between ruptured and unruptured aneurysms. Among shape descriptors, Non-Sphericity Index ($P < 0.0001$, AUC = 0.73), AspectRatio ($P < 0.0001$, AUC = 0.72), and Height/Width ($P < 0.0001$, AUC = 0.71) were best performers (Table 3 and Figure 4A).

Multivariate statistical analysis (Figure 4B) in the bifurcation subset revealed enhanced Radiomics (Elongation, Flatness, MajorAxisLength, SizeRatioHeightOrthogonal, and SizeRatioMaximumDiameter) (AUC = 0.78) outperformed both conventional Radiomics (AUC = 0.74) and established descriptors (AUC = 0.76) (Figure 4C). In this bifurcation subset, enhanced Radiomics performance depended more on inflow parent vessel size estimation than on aneurysm and neck orientation. Because of this dependence on inflow parent vessel, we repeated the univariate and multivariate analysis in this group, using patient-specific inflow vessel measurements as opposed to estimated values. This analysis showed that using estimated location-based inflow vessel values is a good substitute when performing morphological analysis, resulting in no significant difference in performance (0.774 for measured vs. 0.779 for estimated) (Supplemental Tables 1 and 2).

Statistical Analysis on Aneurysms <7 mm

There were 178 aneurysms (48 ruptured) whose SizeMaximum was <7 mm. However, only 5 of these aneurysms were ruptured sidewall aneurysms, which prevented us from performing analysis on the sidewall subset. In the bifurcation group, there were 72 unruptured and 43 ruptured aneurysms. Consequently, univariate and multivariate analysis was performed in this subset of bifurcation aneurysms. Results showed that univariate analysis on this smaller set resulted in very similar statistical performance for all 3 groups of features (established, Radiomics, and

Table 2. Sidewall Aneurysms

Parameter	Aneurysm Unruptured ($n = 103$)	Aneurysm Ruptured ($n = 32$)	*P* Value	AUC
Age, years	54.99 ± 14.41	59.17 ± 16.02	0.16	0.59
Established size and shape descriptors				
SizeMaximum, mm	6.88 ± 3.24	10.35 ± 4.26	<0.0001*	0.77
NeckAverage, mm	4.01 ± 1.47	4.4 ± 1.54	0.1904	0.57
Area, mm^2	96.86 ± 100.49	185.2 ± 149.79	0.0002*	0.72
Volume, mm^3	116.64 ± 185.76	253.91 ± 299.04	0.0019*	0.70
HeightMaximum, mm	5.28 ± 2.78	8.63 ± 3.84	<0.0001*	0.79
WidthMaximum, mm	5.52 ± 2.44	7.26 ± 3.09	0.001*	0.68
Height/Width	0.94 ± 0.2	1.23 ± 0.37	<0.0001*	0.76
AspectRatio	1.32 ± 0.53	2.09 ± 1.13	<0.0001*	0.78
BottleneckFactor	1.49 ± 0.4	1.92 ± 0.78	<0.0001*	0.69
SizeRatio	1.56 ± 0.95	2.83 ± 1.6	<0.0001*	0.81
Non-Sphericity Index	0.17 ± 0.07	0.25 ± 0.08	<0.0001*	0.78
Ellipticity Index	0.26 ± 0.02	0.27 ± 0.02	0.02*	0.63
Undulation Index	0.1 ± 0.07	0.14 ± 0.08	0.01*	0.66
Radiomics descriptors				
Elongation	0.78 ± 0.12	0.68 ± 0.16	0.0002*	0.68
Flatness	0.66 ± 0.11	0.57 ± 0.14	0.0001*	0.71
LeastAxisLength, mm	3.8 ± 1.69	4.97 ± 2.01	0.0011*	0.68
MajorAxisLength, mm	5.97 ± 2.92	9.06 ± 4.05	<0.0001*	0.76
Maximum2DDiameterColumn, mm	6.16 ± 2.93	8.93 ± 3.82	<0.0001*	0.74
Maximum2DDiameterRow, mm	6.27 ± 2.95	8.71 ± 3.8	0.0002*	0.71
Maximum2DDiameterSlice, mm	6.17 ± 2.76	8.45 ± 3.34	0.0001*	0.71
Maximum3DDiameter, mm	6.94 ± 3.25	10.42 ± 4.3	<0.0001*	0.77
MeshVolume, mm^3	117.57 ± 186.81	256.84 ± 303.35	0.0018*	0.70
MinorAxisLength, mm	4.52 ± 2.1	5.96 ± 2.46	0.0012*	0.68
Sphericity	0.79 ± 0.05	0.78 ± 0.05	0.1111	0.62
SurfaceArea, mm^2	124.11 ± 124.16	221.72 ± 172.6	0.0005*	0.71
SurfaceVolumeRatio, 1/mm	1.83 ± 0.86	1.34 ± 0.64	0.0026*	0.69
Enhanced Radiomics descriptors				
HeightOrthogonal	6.59 ± 3.05	9.35 ± 3.39	<0.0001*	0.75
WidthOrthogonal	6.11 ± 2.84	8.06 ± 3.44	0.0011*	0.68
Height/Width Orthogonal	1.09 ± 0.12	1.21 ± 0.24	0.0003*	0.67
SizeRatioHeightOrthogonal	1.91 ± 1.01	2.88 ± 1.18	<0.0001*	0.78
SizeRatioMaximumDiameter	2.01 ± 1.06	3.16 ± 1.36	<0.0001*	0.79

Univariate statistical analysis of established and Radiomics parameters for rupture status discrimination. Values are shown as mean ± SD.
AUC, area under the curve.
*Indicates statistical significance, assumed for $P < 0.05$.

enhanced Radiomics) compared with performance on the entire bifurcation group (**Supplemental Tables 3** and **4**). Repeated multivariate analysis using the features previously selected for the entire bifurcation set (**Figure 4**) resulted in established AUC of 0.79, Radiomics AUC of 0.76, and enhanced Radiomics AUC of 0.78.

Table 3. Bifurcation Aneurysms

Parameters	Aneurysm Unruptured (n = 126)	Aneurysm Ruptured (n = 90)	P Value	AUC
Age, years	57.92 ± 12.61	54.77 ± 15.83	0.10	0.56
Established size and shape descriptors				
SizeMaximum, mm	7.07 ± 2.88	7.93 ± 3.56	0.05	0.56
NeckAverage, mm	4.03 ± 1.33	3.6 ± 1.29	0.01*	0.60
Area, mm^2	98.17 ± 84.65	115.31 ± 119.5	0.21	0.52
Volume, mm^3	111.32 ± 141.27	135.98 ± 216.64	0.31	0.48
HeightMaximum, mm	5.53 ± 2.53	6.5 ± 3.09	0.01*	0.59
WidthMaximum, mm	5.71 ± 2.37	5.67 ± 2.57	0.90	0.52
Height/Width	0.98 ± 0.24	1.17 ± 0.28	<0.0001*	0.71
AspectRatio	1.39 ± 0.53	1.85 ± 0.66	<0.0001*	0.72
BottleneckFactor	1.53 ± 0.41	1.83 ± 0.55	<0.0001*	0.68
SizeRatio	2.24 ± 1.1	3.04 ± 1.53	<0.0001*	0.67
Non-Sphericity Index	0.18 ± 0.1	0.24 ± 0.07	<0.0001*	0.73
Ellipticity Index	0.26 ± 0.02	0.27 ± 0.02	<0.0001*	0.67
Undulation Index	0.11 ± 0.1	0.14 ± 0.09	0.02*	0.65
Radiomics descriptors				
Elongation	0.77 ± 0.13	0.66 ± 0.13	<0.0001*	0.72
Flatness	0.65 ± 0.12	0.56 ± 0.11	<0.0001*	0.73
LeastAxisLength, mm	3.94 ± 1.58	3.86 ± 1.79	0.72	0.53
MajorAxisLength, mm	6.16 ± 2.65	7.1 ± 3.35	0.02*	0.58
Maximum2DDiameterColumn, mm	6.26 ± 2.56	6.89 ± 3.31	0.08	0.54
Maximum2DDiameterRow, mm	6.45 ± 2.64	7.06 ± 3.30	0.30	0.51
Maximum2DDiameterSlice, mm	6.21 ± 2.55	6.54 ± 3.09	0.32	0.53
Maximum3DDiameter, mm	7.13 ± 2.89	8.01 ± 3.58	0.04*	0.56
MeshVolume, mm^3	113.53 ± 142.49	136.15 ± 218.85	0.35	0.50
MinorAxisLength, mm	4.62 ± 1.8	4.56 ± 2.04	0.83	0.53
Sphericity	0.8 ± 0.05	0.77 ± 0.06	<0.0001*	0.67
SurfaceArea, mm^2	124.05 ± 102.49	142.53 ± 147.15	0.29	0.51
SurfaceVolumeRatio, 1/mm	1.69 ± 0.78	1.75 ± 0.73	0.63	0.53
Enhanced Radiomics descriptors				
HeightOrthogonal	6.77 ± 2.73	7.46 ± 3.33	0.09	0.56
WidthOrthogonal	6.21 ± 2.55	6.54 ± 3.09	0.39	0.52
Height/Width Orthogonal	1.06 ± 0.17	1.18 ± 0.24	0.01*	0.57
SizeRatioHeightOrthogonal	2.72 ± 1.44	3.28 ± 1.49	0.002*	0.62
SizeRatioMaximumDiameter	2.87 ± 1.19	3.52 ± 1.54	0.0001*	0.63

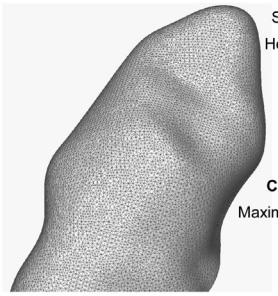
Univariate statistical analysis of established and Radiomics parameters for rupture status discrimination. Values are shown as mean ± SD.
AUC, area under the curve.
*Indicates statistical significance, assumed for $P < 0.05$.

DISCUSSION

It was previously shown that size- and shape-based descriptors perform better at identifying ruptured status in sidewall than in bifurcation aneurysms,[21] with Baharoglu et al.[21] reporting an AUC of 0.87 for rupture classification in sidewall aneurysms, but only 0.67 in bifurcation lesions. This represents a significant

A

Ruptured PCOM Aneurysm



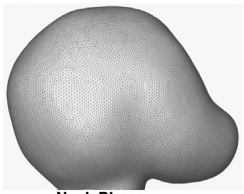
Neck Plane

Established Features
SizeMaximum = 13.54 mm
HeightMaximum = 11.64 mm
Height/Width = 1.49
AspectRatio = 1.65
Non-sphericity = 0.27
Ellipticity Index = 0.29

Conventional Radiomics
Maximum3DDiameter = 13.89 mm
Elongation = 0.61
Flatness = 0.56

Enhanced Radiomics
HeightOrthogonal = 8.6 mm
SizeRatioHeightOrthogonal = 4.16

Unruptured PCOM Aneurysm



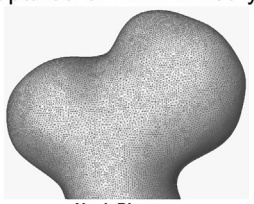
Neck Plane

Established Features
SizeMaximum = 14.12 mm
HeightMaximum = 9.19 mm
Height/Width = 0.69
AspectRatio = 1.42
Non-sphericity = 0.19
Ellipticity Index = 0.23

Conventional Radiomics
Maximum3DDiameter = 14.17 mm
Elongation = 0.79
Flatness = 0.73

Enhanced Radiomics
HeightOrthogonal = 13.63 mm
SizeRatioHeightOrthogonal = 4.24

Ruptured OPHTHA Aneurysm



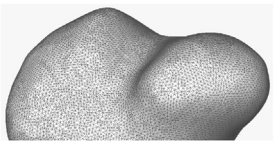
Neck Plane

Established Features
SizeMaximum = 10.08 mm
HeightMaximum = 4.90 mm
Height/Width = 0.89
AspectRatio = 1.67
Non-sphericity = 0.20
Ellipticity Index = 0.25

Conventional Radiomics
Maximum3DDiameter = 10.15 mm
Elongation = 0.67
Flatness = 0.59

Enhanced Radiomics
HeightOrthogonal = 9.86 mm
SizeRatioHeightOrthogonal = 2.81

Unruptured OPHTHA Aneurysm



Neck Plane

Established Features
SizeMaximum = 5.23 mm
HeightMaximum = 3.39 mm
Height/Width = 0.83
AspectRatio = 0.77
Non-sphericity = 0.12
Ellipticity Index = 0.28

Conventional Radiomics
Maximum3DDiameter = 5.25 mm
Elongation = 0.72
Flatness = 0.46

Enhanced Radiomics
HeightOrthogonal = 4.74 mm
SizeRatioHeightOrthogonal = 1.39

B

Multivariate Analysis

Feature	p Value	AUC
Established Descriptors		
Height/Width	0.0006*	
WidthMaximum	0.003*	
Area	0.01*	0.86
EllipticityIndex	0.07	
SizeRatio	0.29	
Radiomics Descriptors		
Maximum3DDiameter	0.002*	
Maximum2DDiameterRow	0.22	
MajorAxisLength	0.11	0.82
SurfaceArea	0.12	
Elongation	0.26	
Enhanced Radiomics Descriptors		
Height/Width Orthogonal	0.0008*	
Maximum3DDiameter	0.01*	
HeightOrthogonal	0.05	0.85
MeshVolume	0.07	
SurfaceArea	0.23	

C

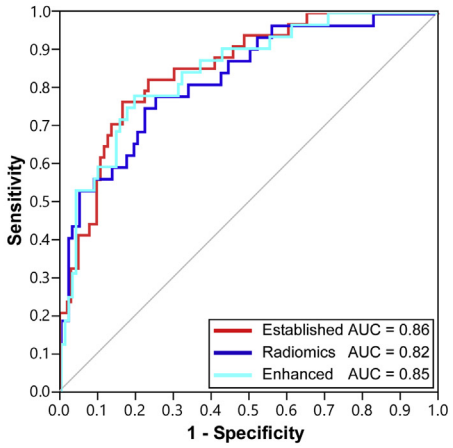
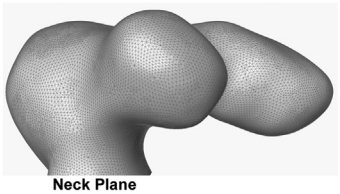


Figure 3. Sidewall aneurysms. (**A**) Ruptured and unruptured sidewall aneurysms. Enhanced HeightOrthogonal is significantly larger in ruptured sidewall aneurysms. (**B**) In multivariate analysis, enhanced predictive performance depended on aneurysm and neck orientation (Height/WidthOrthogonal and HeightOrthogonal) and not on vessel size estimation. (**C**) Area under the curve (AUC) metric of the receiver operating characteristic curve for multivariate statistical analysis. Enhanced Radiomics (AUC = 0.85) outperformed conventional Radiomics (AUC = 0.82) and had a performance similar to that of established features (AUC = 0.86). PCOM, posterior communicating artery; OPHTHA, ophthalmic artery; AUC, area under the curve.

A

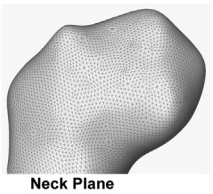
Ruptured ACOM Aneurysm



Neck Plane

Established Features	Conventional Radiomics
SizeMaximum = 7.04 mm	Maximum3DDiameter = 7.08 mm
HeightMaximum = 4.38 mm	Elongation = 0.58
Height/Width = 0.87	Flatness = 0.46
AspectRatio = 1.74	**Enhanced Radiomics**
Non-sphericity = 0.36	Height/Width Orthogonal = 0.74
Ellipticity Index = 0.29	SizeRadioHeightOrthogonal = 2.62

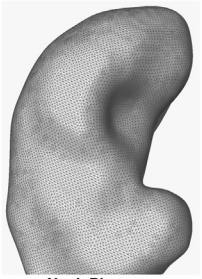
Unruptured ACOM Aneurysm



Neck Plane

Established Features	Conventional Radiomics
SizeMaximum = 3.98 mm	Maximum3DDiameter = 4.02 mm
HeightMaximum = 3.17 mm	Elongation = 0.71
Height/Width = 1.10	Flatness = 0.0.62
AspectRatio = 1.49	**Enhanced Radiomics**
Non-sphericity = 0.18	Height/Width Orthogonal = 1.08
Ellipticity Index = 0.25	SizeRatioHeightOrthogonal = 1.88

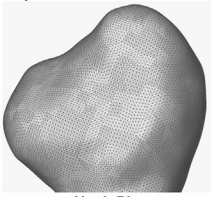
Ruptured MCA Aneurysm



Neck Plane

Established Features	Conventional Radiomics
SizeMaximum = 11.61 mm	Maximum3DDiameter = 11.64 mm
HeightMaximum = 10.62 mm	Elongation = 0.57
Height/Width = 1.40	Flatness = 0.49
AspectRatio = 2.42	**Enhanced Radiomics**
Non-sphericity = 0.30	Height/Width Orthogonal = 1.57
Ellipticity Index = 0.27	SizeRatioHeightOrthogonal = 3.46

Unruptured MCA Aneurysm



Neck Plane

Established Features	Conventional Radiomics
SizeMaximum = 5.63 mm	Maximum3DDiameter = 5.67 mm
HeightMaximum = 4.76 mm	Elongation = 0.98
Height/Width = 0.95	Flatness = 0.77
AspectRatio = 1.34	**Enhanced Radiomics**
Non-sphericity = 0.14	Height/Width Orthogonal = 1.08
Ellipticity Index = 0.24	SizeRatioHeightOrthogonal = 2.12

B

Multivariate Analysis

Feature	p Value	AUC
Established Descriptors		
BottleneckFactor	0.42	
SizeRatio	0.13	
EllipticityIndex	0.0005*	0.76
UndulationIndex	0.07	
Non-sphericity	0.08	
Radiomics Descriptors		
Elongation	0.06	
Flatness	0.27	
MajorAxisLength	0.12	0.74
Maximum3DDiameter	0.11	
Enhanced Radiomics Descriptors		
Elongation	0.15	
Flatness	0.07	
MajorAxisLength	0.0006*	0.78
SizeRatioHeightOrthogonal	0.19	
SizeRatioMaximumDiameter	0.01*	

C

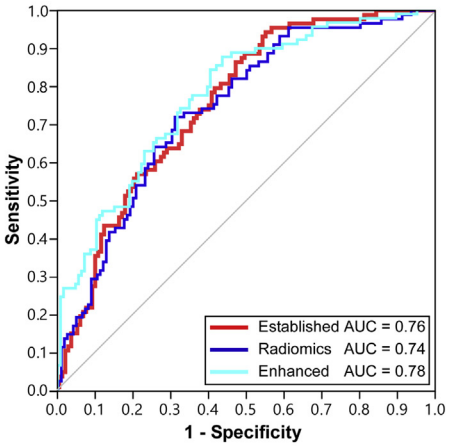


Figure 4. Bifurcation aneurysms. (**A**) Ruptured and unruptured bifurcation aneurysms. Enhanced SizeRatioHeightOrthogonal is significantly larger in bifurcation aneurysms. (**B**) In multivariate analysis, enhanced predictive performance depended on size ratio determination based on estimated vessel size and less on aneurysm orientation. (**C**) Area under the curve (AUC) metric of the receiver operating characteristic curve for multivariate statistical analysis. Enhanced Radiomics (AUC = 0.78) outperformed established features (AUC = 0.76) and Radiomics (AUC = 0.74). ACOM, anterior communicating artery; MCA, middle cerebral artery; AUC, area under the curve.

shortcoming, as bifurcation lesions often rupture at small sizes[27] and represent >50% of all rupture cases. In fact, for smaller aneurysms, bifurcation type alone presents a significant risk factor for growth and progression.[27]

Radiomics-derived descriptors were recently proposed for rupture status prediction of cerebral aneurysms.[8-10] Zhang et al.[9] reported Radiomics Elongation as a predictor for angiographic occlusion status after flow-diverter embolization of cerebral aneurysms. Liu et al.[8] evaluated Radiomics-derived morphological descriptors for prediction of aneurysm stability and identified Flatness as the most important predictor with an AUC of 0.73.

Radiomics for aneurysm morphological evaluation has the advantage of a single platform for the entire image processing pipeline. However, Ludwig et al.[10] found that Radiomics-based Elongation and Flatness were outperformed by established size and shape descriptors for rupture status classification,[10] likely because the latter included data on neck orientation and inflow vessel size, which were lacking in conventional unoriented Radiomics analysis.

In this study, we proposed a simple strategy to recover aneurysm orientation data, by introducing a preprocessing step where, by convention, the neck of the aneurysm was aligned with the XY plane, allowing us to overcome this shortcoming for the evaluation of aneurysmal height, width, and height/width ratios. This orientation process enabled measurement of dome height, previously shown to be a superior denominator over maximal dimension when computing established size and shape descriptors.[23] In addition, we introduced an aneurysm location–dependent inflow vessel size, obviating the need for user measurement of parent vessel dimensions and simplifying a machine-based approach based on dome analysis and a priori location knowledge, thus allowing for the evaluation of size ratios (aneurysms size over inflow vessel diameter).

Overall, enhanced Radiomics outperformed Radiomics descriptors alone for both sidewall (AUC = 0.85 vs. AUC = 0.82) and bifurcation aneurysms (AUC = 0.78 vs. AUC = 0.74); its sidewall performance benefited from the ability to evaluate aneurysm orientation, enabling capture of dome height and height/width leading to improved performance in multivariate analysis. In contrast, its bifurcation performance benefited from the ability to evaluate height and inflow vessel information. Use of SizeRatio based on both maximal size and height resulted in improved performance in multivariate analysis. Although multivariate analysis performance remained higher in sidewall compared with bifurcation aneurysms (AUC = 0.85 vs. AUC = 0.78) across all methods, enhanced Radiomics (AUC = 0.78) outperformed conventional Radiomics (AUC = 0.74) in bifurcation analysis, a significant contribution. Enhanced Radiomics had similar or slightly improved rupture status discrimination power compared with established descriptors both in sidewall (AUC = 0.85 vs. AUC = 0.86) and in bifurcation (AUC = 0.78 vs. AUC = 0.76) subsets.

Aneurysm morphology continues to be intensely studied for rupture risk estimation, but also following endovascular interventions, for monitoring purposes. Despite intense research, the imaging and shape processing pipeline still includes many user-dependent manual and semiautomatic steps as well as use of multiple processing platforms.

PyRadiomics (Radiomics)[1] is a recently introduced automatic imaging processing tool for pixel-by-pixel extraction of object features, including shape-based parameters; however, as currently used, Radiomics underperforms established descriptors (e.g., size, height, height/width, etc.) in discriminating rupture status.[10] Here we proposed a strategy to recover some of these performance differences. Given the performance improvement over Radiomics, the operator-independent methodology, and the simplified processing pipeline, enhanced Radiomics emerges as a strong candidate for larger-scale multicenter and multimodality validation. Prospective studies are required to validate our findings, but the clinical implication of our report, were Radiomics to have a similar or better performance to established feature, is the ability to streamline the aneurysm morphological evaluation pipeline for clinicians and researchers. This novel use of Radiomics for aneurysm morphological analysis opens the possibility for additional applications of Radiomics in intracranial aneurysm evaluation, such as monitoring aneurysms for size and growth progression, and follow-up evaluations after endovascular treatment.

Study Limitations

This study is retrospective in nature, and patients with unruptured aneurysms were not followed over time until subsequent rupture owing to ethical and clinical concerns. Consequently, as with similar retrospective research, the association between ruptured status and aneurysm morphology suggests a correlation, but not causation, a limitation shared with all similar research. In addition, retrospective analysis relies on the hypothesis that aneurysms do not change size and shape after rupture. Conclusive data on this subject are lacking, and although consistent with intraoperative findings, some studies suggest that significant morphological changes do not occur with rupture[28]; were shape to dramatically change after rupture, the current class of analysis would need to be reevaluated. However, our methodology is consistent with relevant literature and similar to all previous work mentioned here. Future prospective studies are required to validate the predictive merit of this analysis.

Furthermore, the inflow parent vessel dimension is estimated from literature reports based on aneurysm location, which may introduce errors in cases with unique parent vessel dysplasia. Whereas the use of patient-specific vessel caliber measurement would be preferred, the purpose of this study was to recover some of the performance discrepancies between established and Radiomics features, while maintaining the relative simplicity and sparse streamlined characteristics of the Radiomics processing pipeline. Although our analysis showed that location-based estimated inflow vessel values were acceptable substitutes for actual values, future studies will explore how intermediary steps can be added to the pipeline to obtain patient-specific vessel measurements based on clinical and research need.

CONCLUSIONS

Enhanced Radiomics with neck orientation and location-dependent parent vessel estimation offers an efficient operator-independent methodology with superior rupture status

classification compared with conventional Radiomics. Its performance is similar to that of more labor-intensive established size and shape descriptors, with the advantage of a simplified, operator-independent processing pipeline. Future work is needed to validate these promising results across imaging modalities and in multicenter large-scale multinational datasets to ascertain generalizability.

CRediT AUTHORSHIP CONTRIBUTION STATEMENT

Alexandra Lauric: Acquisition of data, Image processing, Formal analysis, Data curation, Writing — original draft. **Calvin G. Ludwig:** Acquisition of data, Image processing, Writing — review & editing. **Adel M. Malek:** Conceptualization, Methodology, Acquisition of data, Formal analysis, Data curation, Writing — review & editing, Final approval.

REFERENCES

1. van Griethuysen JJM, Fedorov A, Parmar C, et al. Computational radiomics system to decode the radiographic phenotype. *Cancer Res*. 2017;77:e104-e107.
2. Hyun SH, Ahn MS, Koh YW, Lee SJ. A machine-learning approach using PET-based radiomics to predict the histological subtypes of lung cancer. *Clin Nucl Med*. 2019;44:956-960.
3. Wang K, Lu X, Zhou H, et al. Deep learning Radiomics of shear wave elastography significantly improved diagnostic performance for assessing liver fibrosis in chronic hepatitis B: a prospective multicentre study. *Gut*. 2019;68:729-741.
4. Toivonen J, Montoya Perez I, Movahedi P, et al. Radiomics and machine learning of multisequence multiparametric prostate MRI: towards improved non-invasive prostate cancer characterization. *PLoS One*. 2019;14:e0217702.
5. Fan Y, Chen C, Zhao F, et al. Radiomics-based machine learning technology enables better differentiation between glioblastoma and anaplastic oligodendroglioma. *Front Oncol*. 2019;9:1164.
6. Chen C, Ou X, Wang J, Guo W, Ma X. Radiomics-based machine learning in differentiation between glioblastoma and metastatic brain tumors. *Front Oncol*. 2019;9:806.
7. Zhou Z, Chen L, Sher D, et al. Predicting lymph node metastasis in head and neck cancer by combining many-objective radiomics and 3-dimensional convolutional neural network through evidential reasoning. *Ann Int Conf IEEE Eng Med Biol Soc*. 2018;2018:1-4.
8. Liu Q, Jiang P, Jiang Y, et al. Prediction of aneurysm stability using a machine learning model based on PyRadiomics-derived morphological features. *Stroke*. 2019;50:2314-2321.
9. Zhang Y, Ma C, Liang S, et al. Morphologic feature elongation can predict occlusion status following pipeline embolization of intracranial aneurysms. *World Neurosurg*. 2018;119:e934-e940.
10. Ludwig CG, Lauric A, Malek JA, Mulligan R, Malek AM. Performance of Radiomics derived morphological features for prediction of aneurysm rupture status. *J Neurointerv Surg*. 2021;13:755-761.
11. van Gijn J, Kerr RS, Rinkel GJE. Subarachnoid haemorrhage. *Lancet*. 2007;369:306-318.
12. Wiebers D, Whisnant J, Forbes G, et al. Unruptured intracranial aneurysms—risk of rupture and risk of surgical intervention. *N Engl J Med*. 1998;339:1725-1733.
13. Wiebers DO, Whisnant JP, O'Fallon WM. The natural history of unruptured intracranial aneurysms. *N Engl J Med*. 1981;304:696-698.
14. AlMatter M, Bhogal P, Aguilar Pérez M, et al. The size of ruptured intracranial aneurysms: a 10-year series from a single center. *Clin Neuroradiol*. 2019;29:125-133.
15. Mocco J, Brown RD Jr, Torner JC, et al. Aneurysm morphology and prediction of rupture: an international study of unruptured intracranial aneurysms analysis. *Neurosurgery*. 2018;82:491-496.
16. Hoh BL, Sistrom CL, Firment CS, et al. Bottleneck factor and height-width ratio: association with ruptured aneurysms in patients with multiple cerebral aneurysms. *Neurosurgery*. 2007;61:716-723.
17. Ujiie H, Tamano Y, Sasaki K, et al. Is the aspect ratio a reliable index for predicting the rupture of a saccular aneurysm? *Neurosurgery*. 2001;48:495-502.
18. Rahman M, Smietana J, Hauck E, et al. Size ratio correlates with intracranial aneurysm rupture status: a prospective study. *Stroke*. 2010;41:916-920.
19. Baharoglu M, Schirmer C, Hoit D, Gao B, Malek A. Aneurysm inflow-angle as a discriminant for rupture in sidewall cerebral aneurysms: morphometric and computational fluid dynamic analysis. *Stroke*. 2010;41:1423-1430.
20. Raghavan ML, Ma B, Harbaugh RE. Quantified aneurysm shape and rupture risk. *J Neurosurg*. 2005;102:355-362.
21. Baharoglu MI, Lauric A, Gao BL, Malek AM. Identification of a dichotomy in morphological predictors of rupture status between sidewall- and bifurcation-type intracranial aneurysms. *J Neurosurg*. 2012;116:871-881.
22. Rosato R, Comptdaer G, Mulligan R, et al. Increased focal internal carotid artery angulation in patients with posterior communicating artery aneurysms. *J Neurointerv Surg*. 2020;12:1142-1147.
23. Lauric A, Baharoglu MI, Malek AM. Ruptured status discrimination performance of aspect ratio, height/width, and bottleneck factor is highly dependent on aneurysm sizing methodology. *Neurosurgery*. 2012;71:38-46.
24. Lauric A, Baharoglu MI, Gao BL, et al. Incremental contribution of size ratio as a discriminant for rupture status in cerebral aneurysms: comparison with size, height, and vessel diameter. *Neurosurgery*. 2012;70:944-952.
25. Xiang J, Natarajan SK, Tremmel M, et al. Hemodynamic-morphologic discriminants for intracranial aneurysm rupture. *Stroke*. 2011;42:144-152.
26. Kikinis R, Pieper SD, Vosburgh KG. 3D Slicer: a platform for subject-specific image analysis, visualization, and clinical support. In: Jolesz FA, ed. *Intraoperative Imaging and Image-Guided Therapy*. New York, NY: Springer New York; 2014:277-289.
27. Choi HH, Cho YD, Jeon JP, et al. Growth of untreated unruptured small-sized aneurysms (<7mm): incidence and related factors. *Clin Neuroradiol*. 2018;28:183-189.
28. Asari S, Ohmoto T. Natural history and risk factors of unruptured cerebral aneurysms. *Clin Neurol Neurosurg*. 1993;95:205-214.

Conflict of interest statement: The authors declare that the article content was composed in the absence of any commercial or financial relationships that could be construed as a potential conflict of interest.

Received 6 October 2021; accepted 9 November 2021

Citation: World Neurosurg. (2021). https://doi.org/10.1016/j.wneu.2021.11.038

*Journal homepage: **www.journals.elsevier.com/world-neurosurgery***

*Available online: **www.sciencedirect.com***

1878-8750/$ - see front matter *© 2021 Elsevier Inc. All rights reserved.*

Supplemental Table 1. Performance Comparison of Enhanced Radiomics Features When Using Estimated Parent Vessel versus Actual Parent Vessel Measurements

Parameters	Aneurysm Unruptured ($n = 126$	Aneurysm Ruptured ($n = 90$	*P* Value	AUC
Sidewall aneurysms				
Estimated PV, mm	3.55 ± 0.45	3.32 ± 0.47	0.01*	0.67
Measured PV, mm	3.55 ± 0.73	3.21 ± 0.86	0.02*	
SizeRatioHeightOrthogonal with estimated PV	1.91 ± 1.01	2.88 ± 1.18	<0.0001*	0.78
SizeRatioHeightOrthogonal with measured PV	1.79 ± 1.01	2.67 ± 1.37	0.0001*	0.73
SizeRatioMaximumDiameter using estimated PV	2.01 ± 1.06	3.16 ± 1.36	<0.0001*	0.79
SizeRatioMaximumDiameter using measured PV	2.04 ± 1.14	3.42 ± 1.73	<0.0001*	0.81
Bifurcation aneurysms				
Estimated PV, mm	2.52 ± 0.39	2.28 ± 0.43	<0.0001*	0.67
Measured PV, mm	2.61 ± 0.67	2.23 ± 0.54	<0.0001*	0.61
SizeRatioHeightOrthogonal with estimated PV	2.72 ± 1.44	3.28 ± 1.49	0.002*	0.62
SizeRatioHeightOrthogonal with measured PV	2.47 ± 1.01	3.05 ± 1.47	0.0007*	0.61
SizeRatioMaximumDiameter using estimated PV	2.87 ± 1.19	3.52 ± 1.54	0.0001*	0.63
SizeRatioMaximumDiameter using measured PV	2.86 ± 1.23	3.72 ± 1.71	<0.0001*	0.65

Values are shown as mean ± SD.
AUC, area under the curve; PV, parent vessel.
*Indicates statistical significance, assumed for $P < 0.05$.

Supplemental Table 2. Multivariate Analysis for Bifurcation Aneurysms

Feature	*P* Value	Multivariate AUC
Enhanced Radiomics features using estimated parent vessel size		
Elongation	0.15	
Flatness	0.07	
MajorAxisLength	0.0006*	
SizeRatioHeightOrthogonal	0.19	
SizeRatioMaximumDiameter	0.01*	0.779
Enhanced radiomics features using measured parent vessel size		
Elongation	0.18	
Flatness	0.13	
MajorAxisLength	0.01*	
SizeRatioHeightOrthogonal	0.21	
SizeRatioMaximumDiameter	0.05	0.774

*Indicates statistical significance (assumed for $P < 0.05$).
Performance comparison of enhanced Radiomics features when using estimated parent vessel vs. actual parent vessel measurements.
AUC, area under the curve.

Supplemental Table 3. Bifurcation Aneurysms Smaller than 7 mm

Parameters	Aneurysm Unruptured ($n = 72$)	Aneurysm Ruptured ($n = 43$)	*P* Value	AUC
Age, years	55.83 ± 13.14	55.88 ± 17.92	0.98	0.49
Established size and shape descriptors				
SizeMaximum, mm	5.12 ± 1.25	5.23 ± 1.11	0.66	0.51
NeckAverage, mm	3.34 ± 0.87	2.76 ± 0.12	0.0005*	0.68
Area, mm^2	45.12 ± 21.34	41.91 ±16.33	0.40	0.53
Volume, mm^3	34.06 ± 22.23	26.55 ±14.61	0.06	0.58
HeightMaximum, mm	3.86 ± 1.07	4.22 ±0.16	0.08	0.57
WidthMaximum, mm	4.18 ± 1.19	3.71 ± 0.88	0.04*	0.61
Height/Width	0.94 ± 0.23	1.66 ± 0.28	<0.0001*	0.73
AspectRatio	1.20 ± 0.39	1.65 ± 0.63	<0.0001*	0.75
BottleneckFactor	1.36 ± 0.28	1.58 ± 0.49	0.003*	0.65
SizeRatio	1.66 ± 0.74	2,06 ± 0.85	0.008*	0.67
Non-Sphericity Index	0.14 ± 0.08	0.21 ± 0.06	<0.0001*	0.76
Ellipticity Index	0.26 ± 0.02	0.27 ± 0.02	0.008*	0.65
Undulation Index	0.11 ± 0.07	0.13 ± 0.09	0.13	0.62
Radiomics descriptors				
Elongation	0.79 ± 0.13	0.67 ± 0.12	<0.0001*	0.74
Flatness	0.67 ± 0.12	0.56 ± 0.10	<0.0001*	0.73
LeastAxisLength, mm	2.89 ± 0.80	2.58 ± 0.59	0.03*	0.61
MajorAxisLength, mm	4.39 ± 1.12	4.61 ± 1.20	0.30	0.55
Maximum2DDiameterColumn, mm	4.57 ± 1.69	4.52 ± 1.19	0.84	0.52
Maximum2DDiameterRow, mm	4.67 ± 1.21	4.44 ± 1.06	0.28	0.57
Maximum2DDiameterSlice, mm	4.62 ± 1.23	4.53 ± 1.07	0.70	0.53
Maximum3DDiameter, mm	5.19 ±1.27	5.28 ± 1.11	0.68	0.51
MeshVolume, mm^3	34.46 ± 22.41	26.93 ± 14.79	0.06	0.58
MinorAxisLength, mm	3.40 ± 0.90	3.04 ± 0.66	0.03*	0.62
Sphericity	0.80 ± 0.05	0.78 ± 0.05	0.02*	0.63
SurfaceArea, mm^2	60.39 ± 27.01	53.92 ± 20.76	0.18	0.57
SurfaceVolumeRatio, 1/mm	2.16 ± 0.76	2.28 ± 0.61	0.32	0.60
Enhanced Radiomics descriptors				
HeightOrthogonal	4.93 ± 1.23	4.91 ± 1.07	0.93	0.52
WidthOrthogonal	4.55 ± 1.27	4.23 ± 1.03	0.17	0.57
Height/Width Orthogonal	1.10 ± 0.17	1.19 ± 0.24	0.02*	0.59
SizeRatioHeightOrthogonal	2.01 ± 0.58	2.27 ± 0.61	0.02*	0.63
SizeRatioMaximumDiameter	2.11 ± 0.59	2.43 ± 0.64	0.007*	0.64

Univariate statistical analysis of established and Radiomics parameters for rupture status discrimination. Values are shown as mean ± SD.
AUC, area under the curve.
*Indicates statistical significance, assumed for $P < 0.05$.

Supplementary Table 4. Multivariate Regression for Bifurcation Aneurysms Smaller than 7 mm

Feature	*P* Value	Multivariate AUC
Established descriptors		
BottleneckFactor	0.80	
SizeRatio	0.54	
Ellipticity Index	0.18	
Undulation Index	0.04	
Non-Sphericity Index	0.003	0.79
Radiomics descriptors		
Elongation	0.27	
Flatness	0.31	
MajorAxisLength	0.41	
Maximum3DDiameter	0.31	0.76
Enhanced Radiomics descriptors		
Elongation	0.21	
Flatness	0.35	
MajorAxisLength	0.01*	
SizeRatioHeightOrthogonal	0.63	
SizeRatioMaximumDiameter	0.18	0.78

Multivariate analysis using the features previously selected for the bifurcation group and shown in Figure 4.

AUC, area under the curve.

*Indicates statistical significance, assumed for $P < 0.05$.